01 Jan 2007

Wave Propagation on Power Cables with Special Regard to Metallic Screen Design

R. Papazyan

Per Pettersson

David Pommerenke
Missouri University of Science and Technology, davidjp@mst.edu

Recommended Citation

R. Papazyan et al., "Wave Propagation on Power Cables with Special Regard to Metallic Screen Design," *IEEE Transactions on Dielectrics and Electrical Insulation*, Institute of Electrical and Electronics Engineers (IEEE), Jan 2007.
The definitive version is available at https://doi.org/10.1109/TDEI.2007.344621

Wave Propagation on Power Cables with Special Regard to Metallic Screen Design

R. Papazyan[1]
Royal Institute of Technology (KTH)
SE-100 44 Stockholm, Sweden

P. Pettersson
Vattenfall Utveckling AB
SE-162 87 Stockholm, Sweden

and **D. Pommerenke**
University of Missouri-Rolla (UMR)
Rolla, MO 65409, USA

ABSTRACT

The high frequency properties of coaxial power cables are modeled using time- and frequency-domain numerical simulations. This is required due to the complex helical structure of the outer metallic screen. The finite element (FEM) and finite difference time domain methods (FDTD) have been employed to study the effect of screen spiralization. It is established that this screen design causes a dependence of the cable high frequency characteristics on the surrounding medium. Analytical model based on modal analysis of wave propagation in coaxial cables confirms the numerical observations.

Index Terms - **Attenuation measurement, coaxial transmission lines, electromagnetic coupling, finite element methods, FDTD methods, helices, power cable shielding, velocity measurement.**

1 INTRODUCTION

POWER cables are a major asset to the electrical utilities. Moreover, cable failures are one of the primary reasons for interruption in the electricity supply [1]. Among the failure mechanisms water-treeing has been an important cause for cross-linked polyethylene (XLPE) insulated cables. A diagnostic method has been developed for assessment of the cable insulation condition [2], which method is capable of detecting water treeing and estimating the severity of the degradation. However, the diagnostic criteria evaluates the cable insulation as a whole, while water-treeing can also be a local phenomenon, where only specific sections of the cable have been subjected to degradation. Replacement of only these parts would improve the cable condition and will be considerably more cost-effective as compared to a total cable replacement.

For the purpose of localization the high frequency (HF) properties of both the power cable and the degraded region should be well known and understood. Subsequently time domain reflectometry (TDR) can be used to localize the change of the wave propagation properties caused by the insulation degradation. Water treeing, on the other hand, is often associated with local changes in the surrounding medium, e.g. above circa 60% humidity is required for the development of water trees [3]. Power cables can be directly buried or installed in ducts which can lead to variations in the surrounding conditions of the cable. Therefore, it is important to determine if the localized by TDR change is caused by an insulation change, or by change in the surrounding medium, measured as a result of TDR signal coupling to the surroundings. HF power cable models have been previously developed, [4], but the effect of the surrounding medium has not been accounted for. That motivated an investigation of the effect on the HF characteristics of signal coupling through the nonsolid metallic screen designs, Figure 1. The complexity of the metallic screen design rendered numerical simulations as the most feasible modeling approach.

The purpose of the presented work is to contribute to the understanding of electromagnetic wave propagation in power cables. More specifically it addresses the issue of screen

[1] Present affiliation ABB AB, Corporate Research, Västerås, Sweden

Manuscript received on 1 May 2006, in final form 21 November 2006.

design influence on the wave propagation in the cable and the coupling to the surrounding environment.

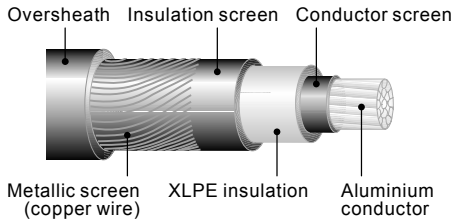

Figure 1. Typical XLPE insulated power cable design for medium voltages.

Areas of applicability of this study are found in localization of insulation degradation along power cables, partial discharge (PD) diagnostics and PD sensor coupling [5-7], data transmission over power networks [8] and transient analysis [9] and a range of electromagnetic compatibility (EMC) studies [10].

2 EXPERIMENTAL OBSERVATIONS

2.1 INVESTIGATED CABLE

A typical design of XLPE insulated power cables can be seen in Figure 1. In this paper simulations and measurements were conducted on a 12/7 kV rated cable with a conductor cross-section of 95 mm^2. The measured cable sample had a length of 5 m. The metallic screen consists of 44 separate helically wound copper wires.

2.2 MEASUREMENT RESULTS

The objective of the experiment is to estimate the effect of two different types of surrounding media – air and water. The cable is placed in a plastic tube that is filled with either air or tap water to control the surrounding medium.

A measurement technique using a Network Analyzer (NA) is applied for extraction of the cable wave propagation constant $\gamma = \alpha + j\beta$ (m^{-1}) given by its real part – attenuation constant α (Np/m) and imaginary part – phase constant β (rad/m) [11]. The phase velocity v (m/s) can then be defined as $v=\omega/\beta$, where ω is the angular frequency. A noticeable increase in the measured attenuation constant can be observed above 70 MHz when the surrounding medium is water, Figure 2. The velocity is however not considerably affected.

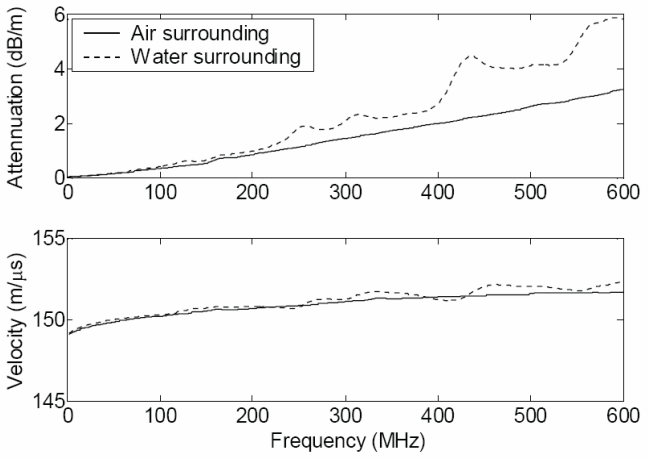

Figure 2. Measured attenuation constant (α) and velocity (ν) for the two types of cable surrounding media: air and water.

3 NUMERICAL MODELS

Since the analytical model in [4] does not account for the cable surrounding medium and spiralization of the metallic screen, these should be taken into account in order to accurately reproduce the experimental results. Because of the complexity of the metallic screen, analytical field theory or circuit approximations analysis become difficult and therefore numerical modeling is considered as a feasible approach. A number of techniques have been developed for numerical electromagnetic field analysis.

A general approach is to obtain second order differential equations for the electric and magnetic field, known as the vector Helmholtz equation or the wave equation. This is the most general and complex equation form for describing the propagation of electromagnetic fields. One can then solve this equation directly in time domain or for sinusoidal time variation at a given frequency. Numerical techniques applying both approaches will be used in this study.

3.1 2D FEM MODEL

The FEM technique originated in the structural analysis [12] and it was applied to electromagnetic problems in the late 1960s [13].

Since then it gained a lot of momentum due to its applicability to complex geometries, inhomogeneous structures and non-linear material characteristics. The FEM technique is used here as a frequency domain method [14].

In this study FEM was used to investigate a 2D cable model. Due to the radial symmetry of the cable geometry certain simplifications in the cable model could be achieved. A quarter of the cable cross section was modeled using two symmetrical boundaries (left and bottom), Figure 3. A 2D model incorporates the assumption of an infinitely long cable with metallic screen wires running parallel to the inner conductor, i.e. the screen spiralization was not included and only the effect of screen wire separation can be investigated with the model. Additionally the model does not take into account the skin losses in the conductor, since these were shown to be negligible as compared to the dielectric losses in the investigated frequency range [4].

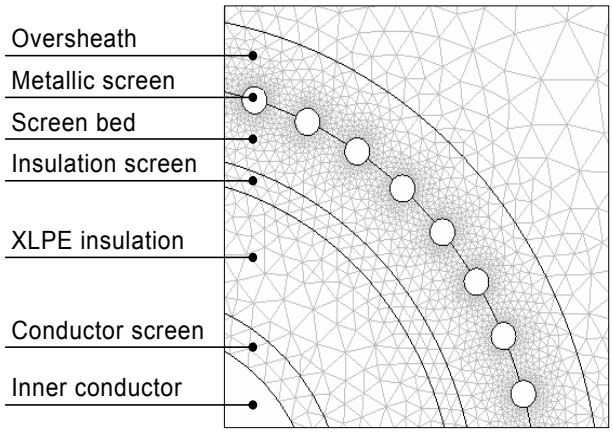

Figure 3. Geometry and mesh structure used in the 2D FEM model. In the investigated cable an additional semi-conducting layer, called screen bed, was used for longitudinal water tightness of the cable construction.

3.2 3D FDTD MODEL

Formulating electromagnetic field problems by means of this technique is appealing due to the simplicity of the approach. It was introduced to the EM computations in 1966 [15]. The method solves the field equation in a finite difference form, and yields a robust and fast algorithm (basically no matrix has to be formed and inverted).

Furthermore to get the result in a certain frequency band one can apply a pulse excitation. A frequency domain method – on the contrary – needs runs performed for each of the desired frequencies.

The FDTD code was used in this investigation because of the time domain simulation, relevant to the application of the broadband TDR technique. The availability of 3D helixes from the graphical user interface [16], which were needed for modeling the cable metallic screen, was also an important advantage.

The meshing of the FDTD cable model required a good balance between precision, computational cost and software restrictions. The longitudinal grid cell size was determined on the basis of the software limit of 400 cells in any direction. This cell size had to be chosen such that it both correctly represents the spiralization of the metallic screen and also allows a sufficiently long cable to be modeled within the 400 cells restriction. The effect of different cell dimensions on the precision of the helix representation can be seen in Figure 4.

The chosen cell size of 1 mm allowed a length of 0.225 m to be modeled, corresponding to one full turn of the screen helix.

Another software constraint was the maximum number of cells in the 3D computational domain which should not exceed 10 million. The transverse cell dimensions were determined by that limitation and by the size of the screen wires cross-section, Figure 5.

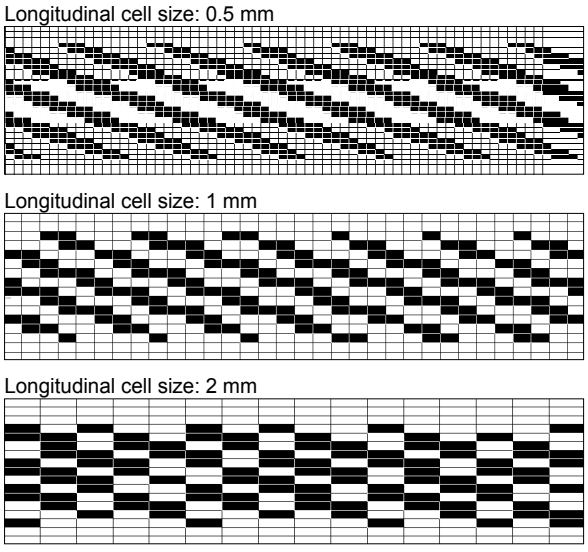

Figure 4. The effect of different longitudinal cell dimensions on the precision of helix representation. At 2 mm the separate helix wires have common edges and corners representing a short circuit between the separate wires. 1 mm cell size was chosen for the present model.

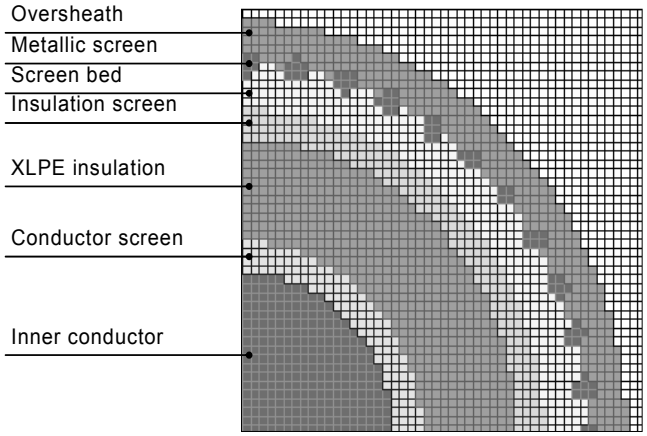

Figure 5. Transverse cross-section of the 3D FDTD cable model corresponding to a total of 6.8 million elements in the 3D computational domain.

The effect of the cell size on the precision of the calculation was also taken into account. While the 2D FEM model calculation took approximately 1 to 3 minutes on a 2.4 GHz, 1 GB RAM personal computer, a 3D model calculation time of 10 hours is typical for models of such complexity and size. Therefore, the size of the computational domain was balanced against the computational cost. The relation between the simulation precision and size of the model can be seen in Table 1.

Since the purpose of this investigation is to estimate the relative effect of the screen design on the propagation parameters, a certain deviation in the absolute precision of the simulations does not compromise the objectives of the study. The robustness and acceptable computational cost of the FDTD method were additional advantages considered for this study.

The model with 6.8 million cells was therefore preferred because of the shorter calculation time of circa 8 hours, as compared to circa 11 hours for the model with 9.1 million elements. The chosen model had a transverse cell size of 0.3x0.3 mm that adequately represented the screen wires cross-section, Figure 5. A 3D representation of the FDTD model of the helical metallic screen and inner conductor is given in Figure 6.

3.3 COMPARISON OF NUMERICAL MODELS

To assure the credibility of the subsequent simulations, results from the two numerical solvers were initially compared to an analytical transmission line model [4], Table 2.

Table 1. Effect of different cell size for the computation of cable losses. 3D FDTD simulations on a cable with air as surrounding medium.

@ 100 MHz	Measurement	3.4 M cells	6.8 M cells	9.1 M cells
Attenuation constant (dB/m)	0.335	0.456	0.433	0.401

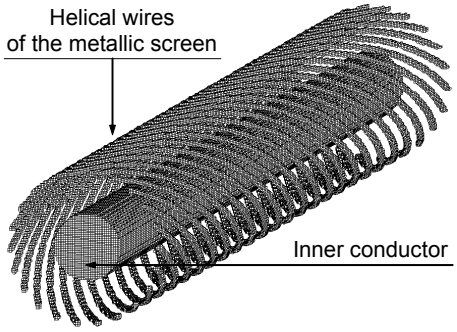

Figure 6. FDTD model of the inner conductor and metallic screen of the power cable. The dielectric layers of the cable insulation are not shown here for clarity of presentation of the helical structure, but are included in the simulation. Radius of the inner and outer conductors is 5.5 mm and 11.75 mm, respectively.

Table 2. Comparison of measurement and model results for the attenuation constant (α) at 100 MHz. FEM and FDTD models assume air as a surrounding medium.

@ 100 MHz	Measurement	Analytical model	Numerical models	
			FEM	FDTD
Attenuation constant (dB/m)	0.335	0.358	0.359	0.433

The comparison reveals marked agreement between the analytical and FEM model results, both matching the measurement result closely. The FDTD result contains relatively higher error, which is attributable mainly to the previously discussed volume discretizing (meshing) and the finite length of the used cable model [17]. The fact that the FDTD model uses a spiralized screen also contributes to the increased attenuation, which will be discussed later in this paper.

4 SIMULATION RESULTS

4.1 DIELECTRIC PROPERTIES USED IN THE SIMULATION

The power cable frequency dependent properties can be found in [4]. Water with real relative permittivity (ε_r) equal to 81 and conductivities of 1E-6, 1E-3 (tap water) and 1 S/m were used. Soil was modeled with $\varepsilon_r = 10$ and conductivities of 1E-6, 1E-3 and 1 S/m [18].

4.2 PROBLEM FORMULATION

Two specific coupling mechanisms have to be investigated in order to construct a complete model of the wave propagation in a cable with a helically wound metallic screen: 1) leakage of the field through the wires and 2) longitudinal magnetic field coupling from the spiralization of the screen.

4.2.1 INFLUENCE OF THE SEPARATION OF THE SCREEN WIRES

Figure 7 presents the equipotential line distribution at two frequencies, 100 MHz and 300 MHz. A frequency dependence of the leakage can be observed with increased potentials outside the cable at higher frequencies.

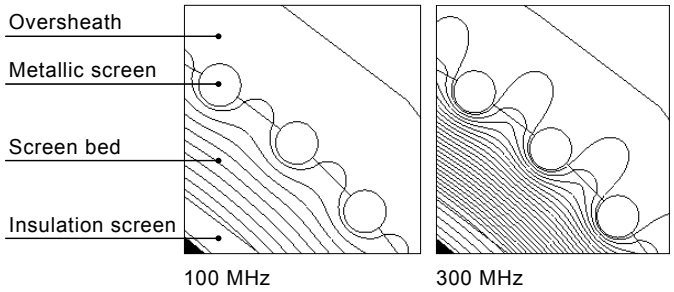

Figure 7. Equipotential line distribution around the metallic screen wires at 100 MHz and 300 MHz. Field leakage past the wired screen increases with frequency.

However, the effect of this phenomenon on the signal attenuation is negligible. No significant difference could be seen when changing the surrounding medium from air to tap water, Figure 8. Additionally, Figure 8 reveals a good agreement between the analytical model from [4] and the 2D FEM simulations.

A 2D FEM model was used for the results in order to isolate the screen wires separation effects, presented in the radial cable cross-section, from the screen wires spiralization, which is a cable geometry feature in the axial direction.

4.2.2 INFLUENCE OF THE SPIRALIZATION OF THE SCREEN WIRES

The longitudinal magnetic field coupling from the spiralization of the screen can only be presented in 3D. The FDTD model is therefore used to study the effect of the helical metallic screen on the propagation of electromagnetic waves along the cable length.

To investigate its effect the cable with a spiralized screen is compared to a solid screen one. The inner conductor and all dielectric layers in the cable construction are identical for the two models.

In this investigation the surrounding medium is air. The simulation results are presented in terms of a Gaussian pulse propagating along two equally long cables sections (0.225 m) with different types of screens, Figure 9. The length of 0.225 m corresponds to one full turn of the screen helix. All measurement and modeling results are scaled to values of 1 meter of cable, in order to be comparable, and therefore length of measured or modeled cable sections is not decisive. However, the length of 0.225 m was chosen with the purpose to present the physical phenomenon related to screen spiralization in its completeness, and on the other hand minimize computational cost.

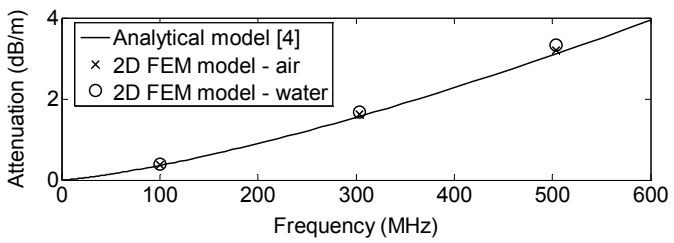

Figure 8. Attenuation constant from an analytical model presented in [4] and 2D FEM simulations for two types of cable surrounding media: air and tap water.

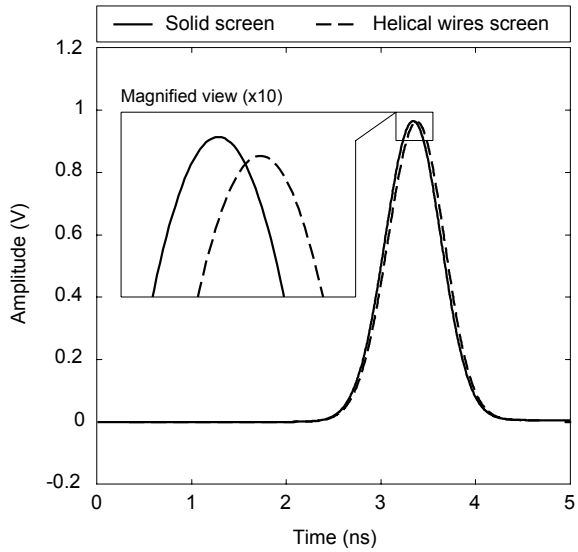

Figure 9. Propagation of Gaussian pulses along cables with different types of metallic screens – solid and helically spiralized.

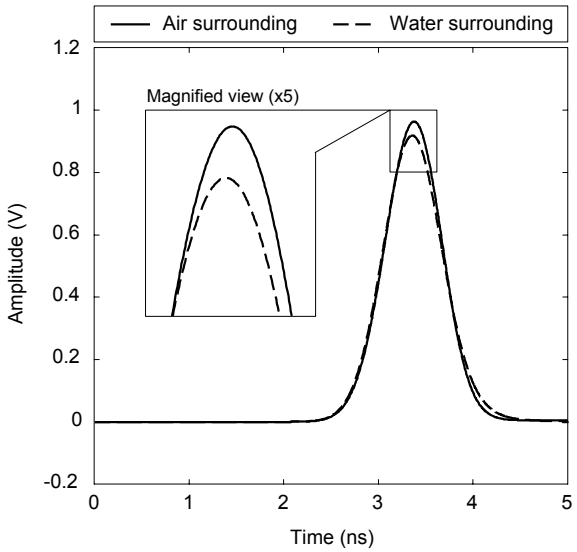

Figure 10. FDTD simulation of a Gaussian pulse propagation along a cable with different types of surrounding media – air and water.

It can be observed that the screen design does not significantly affect cable losses in this case with very similar results for a solid and spiralized metallic screens. In the case of a helical screen, a somewhat longer propagation time and higher damping can be observed. This can be attributed to the longer propagation path for the signal following the spiralized screen. The difference in the velocity and signal attenuation is, however, below 2%, while the length of the spiralized screen is 5.2% longer than the actual cable length. Referring to the relation for velocity $v=1/\sqrt{(LC)}$ this effect can be explained by the increased inductance in the return path of the signal. It is concluded that the screen spiralization would have an insignificant effect on the velocity of propagation and signal attenuation.

The influence of the surrounding medium changes are simulated by replacing air with water (ε_r = 81, σ=0.001 S/m). Figure 10 reveals that there is an influence of the surrounding medium which effects can be represented only using the helical wire screen model.

It should be noted that it is the signal damping that is mainly affected by the surrounding variations. That effect is caused by the longitudinal magnetic field coupling and has its root at the circumstance that metallic screen currents are forced to follow a spiral path, thereby giving raise to longitudinal magnetic field vector components outside and inside the screen. This is a known phenomenon in the practice of telecommunication cables, and an analysis for screens of band type is found in [19], which is referenced in [20].

A comparison of the simulation and measurement results is presented in Figure 11 in terms of increase of signal attenuation after replacing the air surrounding with water.

5 SENSITIVITY ANALYSIS

In this Section the influence of both the screen design parameters and the dielectric properties of the surrounding medium will be investigated.

5.1 INFLUENCE OF THE HELIX PARAMETERS

The influence of the length of one helix turn (p) was studied, Figure 12. Its effect on the dependence of the cable parameters to different surrounding environments is presented in Figures 13 and 14.

5.2 INFLUENCE OF THE SURROUNDING MEDIUM DIELECTRIC PARAMETERS

Figures 13 and 14 also reveal the dependence of the cable properties on the type of surrounding media. It is concluded that the influence is increasing both with frequency and with the increasing value of the relative permittivity of the medium.

A study has also been conducted relating the increase in signal attenuation with the conductivity of the surrounding medium, Figures 15 and 16. The observed dependence of the cable characteristics on the conductivity of the surrounding medium is relatively low.

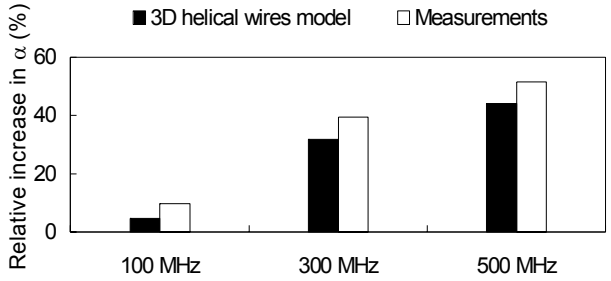

Figure 11. Effect on the attenuation constant when changing the surrounding medium from air to water.

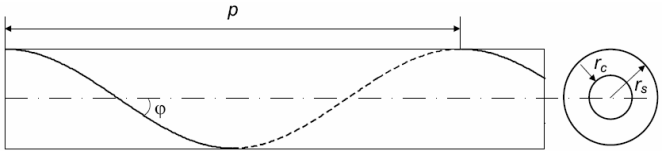

Figure 12. Geometrical parameters of the cable helical screen.

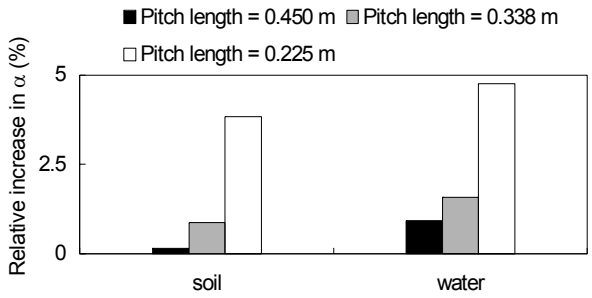

Figure 13. Increase in signal attenuation at 100 MHz after replacing the air surrounding with water (ε_r = 81, σ=0.001 S/m) and soil (ε_r = 10, σ=0.001 S/m). The effect is given for screen designs with different spiral pitch angles.

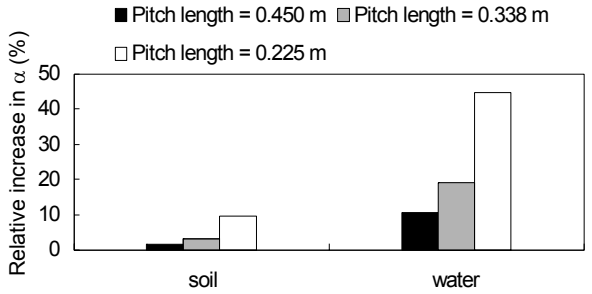

Figure 14. Increase in signal attenuation at 500 MHz after replacing the air surrounding with water (ε_r = 81, σ=0.001 S/m) and soil (ε_r = 10, σ=0.001 S/m). The effect is given for screen designs with different spiral pitch angles.

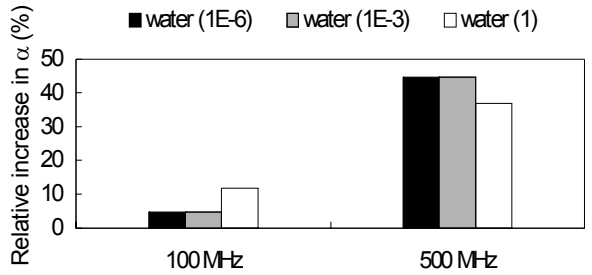

Figure 15. Increase in the attenuation at 100 MHz and 500 MHz after replacing the air surrounding with water (ε_r = 81) with conductivities 1E-6, 1E-3 and 1.

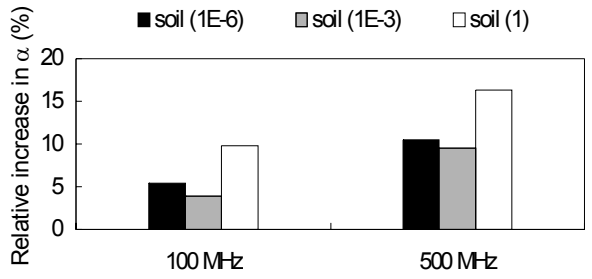

Figure 16. Increase in the attenuation at 100 MHz and 500 MHz after replacing the air surrounding with soil (ε_r = 10) with conductivities 1E-6, 1E-3 and 1.

6 MODAL ANALYSIS AND NUMERICAL MODEL VERIFICATION

The Appendix contains a modal theory of the wave propagation on a coaxial cable situated in an infinite surrounding. Two propagation modes, inner and outer, are identified, where the inner mode is of interest here.

Depending on the type and design of the cable, there will be a coupling to the exterior through the metallic screen and currents will flow in the surrounding and thereby contribute to the attenuation which otherwise comes from ohmic losses in the conductors and dispersive losses in the insulation system. This coupling is reflected in the model by the metallic screen transfer series impedance.

For the screen type and frequency range of interest here, two kinds of coupling mechanisms are identified: leakage of the field past the wires and longitudinal magnetic field coupling from the spiralization of the screen.

The leakage coupling is independent of the spiralization, i.e. it is present even in metallic screens with wires running parallel to the inner conductor. From [19] the geometric factor Λ_{tl} of its inductance, as defined in the Appendix, is given by:

$$\Lambda_{tl} = \frac{1}{n} \ln \frac{r_s^n - r_c^n}{r_s^n - (r_s - \rho)^n} \tag{1}$$

where r_c and r_s are the radii of the inner conductor and screen, respectively, and ρ and n is the radius and number of the screen wires.

Assuming that a tight wire screen behaves like a band with the same pitch of spiralization, the following expression for the associated coupling inductance geometric factor Λ_{ts} may be given.

$$\Lambda_{ts} = \frac{1}{2}\left[1 - \left(\frac{r_c}{r_s}\right)^2\right] \tan^2 \varphi \qquad \varphi = \arctan \frac{2\pi r_s}{p} \tag{2}$$

where p is the pitch of the spiral.

What remains is to give an approximate expression for the contribution to the total attenuation by the signal coupled and propagating in the cable environment α_{env} (Appendix).

$$\alpha_{env} \approx -\frac{\omega}{2\nu_i} \cdot \frac{1}{\Lambda_i} Im \frac{(\delta_t + \Lambda_t)^2}{\Lambda_t + \Lambda_j (1 - \varepsilon_i/\varepsilon_j) + P(1 - \varepsilon_i/\varepsilon_e)} \tag{3}$$

with indices i, j and e denoting insulation, jacket and environment (surrounding), respectively. It has been established that this modal analysis model agrees quantitatively with the numerical simulations up to approximately 100 MHz. Table 3 presents a comparison of the 3D FDTD model and modal analysis model results at 100 MHz. The observed agreement will be elaborated in the following Section.

7 DISCUSSION

Numerical modeling requires a good balance between accuracy and computational cost. It should be noted that the FEM numerical solver placed more stringent requirements on the PC RAM usage, while for the FDTD code simulation times were significantly affected by the PC processor speed [17]. Geometry discretization, truncation of free space, model size restrictions and choice of material properties were some of the variables to be considered. Additionally one turn length of the screen helix could be represented by the 3D numerical model which represented 5% of the measured cable length.

The combined effects of these factors caused some of the deviations between the simulation and measurement results, Figure 11.

Table 3. Relative increase of the attenuation after replacing the air surrounding with water (ε_r = 81, σ=0.001 S/m). Results from numerical and analytical models.

@ 100 MHz	3D numerical model	Modal analysis model
Δα (%)	5.2	4.9

The assumption in the modal analysis of infinite surrounding and infinite cable length were also contributing factors, such that agreement between the analytical and numerical model results was achieved up to approx. 100 MHz.

The sensitivity analysis revealed a significant dependency on the pitch of the screen spiralization, Figures 13 and 14. This strong dependence is elucidated in equations (2) and (3) where the parameter Λ_{ts} contains the pitch angle in $tan2\varphi$, while Λ_{ts} is included to the power of 2 in the numerator of equation (3). Figures 13 and 14 also reveal that the change in signal damping is sensitive to the relative permittivity of surrounding medium and that the dependence increases with the frequency of the signal. On the other hand, the cable damping is not significantly affected by the variations in the conductivity, despite a change of 3 orders of magnitude, Figures 15 and 16.

8 CONCLUSIONS

The cable wave propagation characteristics above approximately 70 MHz can notably be influenced by the surrounding medium. The signal attenuation is predominantly affected by the phenomenon, while the velocity of wave propagation is not significantly altered. It has been established that the dependence is caused by the spiralization of the cable metallic screen. 3D FDTD numerical simulations and analytical modeling based on modal analysis of wave propagation have been used to confirm the experimental observations. It has been established that the variations in cable damping are most sensitive to the pitch of screen spiralization. Changes in the relative permittivity of the surrounding medium also influence signal attenuation, i.e. the type of surrounding medium can be estimated from the measurements. The spiralization of the metallic screen additionally increases the electrical length of the cable due to the higher inductance in the return path. This increase is below 2% in the presented case.

APPENDIX

Let the two-dimensional vectors $V=(V_1, V_2)$ and $I=(I_1, I_2)$ be the voltages and currents of the core-screen, index 1, and screen-ground, index 2, circuits. Then with Z and Y denoting the unit length series impedance and shunt admittance parameter matrices of dimension two

$$ZI + \frac{dV}{dz} = 0 \qquad YV + \frac{dI}{dz} = 0 \tag{A1}$$

where z is the longitudinal coordinate. Using standard matrix eigenvalue theory, equation (A1) has two independent vector solutions

$$V = ae^{\pm\gamma z}V_\gamma \tag{A2}$$

where a is an arbitrary scalar. The two eigenvalues γ^2 are the two solutions of the equation

$$\det(M - \gamma^2 E) = 0 \qquad M = ZY \tag{A3}$$

with E denoting the identity matrix. The solutions are

$$\gamma^2 = \frac{M_{11} + M_{22}}{2} \pm \sqrt{\left(\frac{M_{11} - M_{22}}{2}\right)^2 + M_{12}M_{21}} \tag{A4}$$

For the present study the following unit length parameters may be used

$$\begin{aligned} Z_{11} &= \frac{j\omega\mu_0}{2\pi}\left(\delta_c + \Lambda_i + \delta_s + \Lambda_t\right) & Y_{11} &= \frac{j\omega\varepsilon_0 2\pi}{\Lambda_i/\varepsilon_i} \\ Z_{12} = Z_{21} &= -\frac{j\omega\mu_0}{2\pi}\left(\delta_t + \Lambda_t\right) & Y_{12} = Y_{21} &= 0 \\ Z_{22} &= \frac{j\omega\mu_0}{2\pi}\left(\Lambda_t + \delta_s + \Lambda_j + P\right) & Y_{22} &= \frac{j\omega\varepsilon_0 2\pi}{\left(\frac{\Lambda_j}{\varepsilon_j} + \frac{P}{\varepsilon_e}\right)} \end{aligned} \tag{A5}$$

Here, the δ-complex quantities represent conductor resistances taking account of skin effects, with index c and s denoting core and screen, respectively, and t transfer between the inner and outer circuits. The real Λ-quantities represent inductance related geometric factors, [19], with index i, j and t denoting insulation, jacket (oversheath) and transfer, respectively.

The ε-factors are complex relative permittivities, with indices i, j and e denoting primary insulation, jacket and environment (surrounding), respectively. Semi-conducting layers are incorporated in ε_i, where $\varepsilon=\varepsilon'-j\varepsilon''$. Finally P (complex) represents the inductance of the surrounding.

More specifically δ_c and δ_s are inverse proportional to $\sqrt{(j\omega)}$ for high frequencies, where ω is the angular frequency. Λ_i and Λ_j are the geometric factors connected with cylindrical capacitors, i.e. with r_c, r_s and r_j denoting radius of conductor, screen and jacket, respectively.

$$\Lambda_i = \ln\frac{r_s}{r_c} \qquad \Lambda_j = \ln\frac{r_j}{r_s} \tag{A6}$$

The quantity P is modeled as

$$P = \frac{K_0(y)}{yK_1(y)} \qquad y = r_j\gamma_0\sqrt{\varepsilon_e - \varepsilon_i} \qquad \gamma_0 = j\omega\sqrt{\mu_0\varepsilon_0} \tag{A7}$$

where K_0 and K_1 are the modified Bessel functions of second kind of order zero and one. This assumes the cable placed in infinite ground. The quantities δ_t and Λ_t depend on the type and design of the cable screen.

Now, performing the matrix multiplications ZY gives

$$\begin{aligned} M_{11} &= \gamma_0^2 A & M_{12} &= -\gamma_o^2 B \\ M_{21} &= -\gamma_0^2 C & M_{22} &= \gamma_0^2 D \end{aligned} \tag{A8}$$

where

$$A=\frac{\delta_c+\Lambda_i+\delta_c+\Lambda_t}{\Lambda_i/\varepsilon_i} \qquad B=\frac{\delta_t+\Lambda_t}{\Lambda_j/\varepsilon_j+P/\varepsilon_e}$$
$$C=\frac{\delta_t+\Lambda_t}{\Lambda_i/\varepsilon_i} \qquad D=\frac{\Lambda_t+\delta_s+\Lambda_j+P}{\Lambda_j/\varepsilon_j+P/\varepsilon_e} \tag{A9}$$

Equation (A4) can now be written as

$$\gamma^2=\gamma_0^2\left(\frac{A+D}{2}\pm\sqrt{\left(\frac{A-D}{2}\right)^2+BC}\right) \tag{A10}$$

It is supposed that the transfer effects are rather small so that the second term under the root-sign is dominated by the first one then

$$\gamma_1^2\approx\gamma_0^2\left(A+\frac{BC}{A-D}\right) \qquad \gamma_2^2\approx\gamma_0^2\left(D-\frac{BC}{A-D}\right) \tag{A11}$$

are the two eigevalues. It is realized that the first eigenvalue is associated with an inner mode, primarily propagating inside the cable, and the second one to an outer mode, primarily propagating in the cable surrounding. The propagation constant of the inner mode can further be approximated as

$$\gamma_1\approx\gamma_0\left(\sqrt{A}+\frac{BC}{2\sqrt{A}\left(A-D\right)}\right) \tag{A12}$$

Regarding attenuation, there are in principle three contributions: one due to resistance in the core and screen, one due to the insulation (including semi-conductive layers), and one due to the coupling to the cable environment. Writing $\gamma=\alpha+j\beta$, where α is the unit length attenuation in Nepers, with obvious denotations

$$\alpha\approx\alpha_{cnd}+\alpha_{ins}+\alpha_{env}$$
$$\alpha_{cnd}\approx-\frac{\omega}{2\nu_i}\cdot\frac{1}{\Lambda_i}Im\left(\delta_c+\delta_s\right)$$
$$\alpha_{ins}\approx\frac{\omega}{2\nu_i}\tan\partial_i \qquad \nu_i=\frac{\nu_0}{\sqrt{\varepsilon_i'}} \tag{A13}$$
$$\alpha_{env}\approx-\frac{\omega}{2\nu_i}\cdot\frac{1}{\Lambda_i}Im\frac{\left(\delta_t+\Lambda_t\right)^2}{\Lambda_t+\Lambda_j\left(1-\varepsilon_i/\varepsilon_j\right)+P\left(1-\varepsilon_i/\varepsilon_e\right)}$$

where $\tan\partial_i$ denotes the loss tangent of the cable insulation. It should be noted that the terms α_{cnd} and α_{ins} are identical with these in the model presented in [4].

REFERENCES

[1] L. Bertling, R. Eriksson, R.N. Allan, L.Å. Gustafsson and M. Åhlén, "Survey of Causes of Failures Based on Statistics and Practice for Improvements of Preventive Maintenance Plans", Proc. 14th Power Systems Computation Conf. PSCC'02, Session 13, Paper 2, pp. 1-7, 2002.

[2] P. Werelius, P. Tharning, R. Eriksson, B. Holmgren and U. Gäfvert, "Dielectric spectroscopy for diagnosis of water tree deterioration in XLPE cables", IEEE Trans. Dielect. Elect. Insul., Vol. 8, pp. 27-42, 2001.

[3] B. Holmgren, "Dielectric Response, Breakdown Strength and Water Tree Content of Medium Voltage XLPE Cables", Tech. Lic., Royal Institute of Technology (KTH), TRITA-EEA-9705, Stockholm, Sweden, 1997.

[4] G. Mugala, R. Eriksson, U. Gäfvert and P:Pettersson, "Measurement technique for high frequency characterization of semi-conducting materials in extruded cables", IEEE Trans. Dielect. Elect. Insul., Vol. 11, pp. 471-480, 2004.

[5] G. C. Stone and S. A. Boggs, "Propagation of Partial Discharge Pulses in Shielded Power Cable", IEEE Conf. Electr. Insul. Dielect. Phenomena, pp. 275-280, 1982.

[6] R. Villefrance, J.T. Holboll and M. Henriksen, "Estimation of medium volt-age cable parameters for PD-detection", IEEE Symp. Elect. Insul., Vol. 1, pp. 109-112, 1998.

[7] V. Dubickas and H. Edin, "Couplers for on-line time domain reflectometry diagnostics of power cables", IEEE Conf. Electr. Insul. Dielectr. Phenomena, pp. 210-214, 2004.

[8] I. Froroth, "Broadband accesses communications on power cables", Conf. Networks & Optical Communications NOC' 98, pp. 105-113, 1998.

[9] B. Gustavsen, J. Sletbak and T. Henriksen, "Calculation of electromagnetic transients in transmission cables and lines taking frequency dependent effects accurately into account", IEEE Trans. Power Delivery, Vol. 10, pp. 1076-1084, 1995.

[10] L.-M. Zhou and S. Boggs, "Effect of high frequency cable attenuation on lightning-induced overvoltages at transformers", IEEE Rural Electric Power Conf., , pp. 1-7, 2002.

[11] R. Papazyan, P. Pettersson, H. Edin, R. Eriksson and U. Gäfvert, "Extraction of the High Frequency Power Cable Characteristics from S-parameter Measurements", IEEE Trans. Dielect. Elect. Insul., Vol. 11, pp. 461-470, 2004.

[12] A. Hoorfar and Y. Jamnerjad, "Electromagnetic Modeling and Analysis of Wire-less Communication Antennas", IEEE Trans. Microwave, Vol. 12, pp. 51-67, 2003.

[13] J. Jin, *The Finite Element Method in Electromagnetics*, 2nd ed., New York, Willey, 2002.

[14] FEMLAB FEM code from COMSOL AB, Version 3.0a.

[15] K. S. Yee, "Numerical Solution of Initial Boundary Value Problems involving-Maxwell's equations in isotropic media", IEEE Trans. Antennas Propagat., Vol. 14, pp. 302-307, 1966.

[16] Fidelity FDTD code from Zeland software, Version 4.11.

[17] D. Pommerenke and S. Sakaguchi, "Application of Maxwell Solvers to PD Propagation – Part I: Concepts and Codes", IEEE Electr. Insul. Mag., Vol. 18, No. 5, pp.15-21, 2002.

[18] J.O. Curtis, "Moisture effects on the dielectric properties of soils", IEEE Trans. Geosci. Remote Sensing, Vol. 39, pp. 125-128, 2001.

[19] H. Kaden, *Wirbelströme und Schirmung in der Nachrichtentechnik*, Springer-Verlag, Berlin, Ch. 7, 1959.

[20] E.F. Vance, *Coupling to Shielded Cables*, John Wiley and Sons, New York, Ch. 4, 1978.

Ruslan Papazyan (S'03-M'06) received the M.Sc. degree from the Technical University of Sofia, Bulgaria in 2000 and the Ph.D. degree in electrical engineering from the Royal Institute of Technology (KTH), Sweden, in 2005. He is currently with ABB AB, Corporate Research. His research interests include cable and cable accessories design, cable diagnostics and high frequency properties and modeling of electric power equipment.

Per Pettersson (M'90) received the M.Sc. degree in electrical engineering from the Chalmers Institute of Technology, Sweden in 1967, and in 1973 the Technical Licentiate degree in mathematical statistics from the same institute. He received the Ph.D. degree in electrical plant engineering from the Royal Institute of Technology (KTH), Sweden, in 1995. Dr. Pettersson is presently with Vattenfall Utveckling AB as a Senior Research Engineer.

David Pommerenke (SM'92) received his diploma and the Ph.D. degree from the Technical University Berlin, Germany. He joined Hewlett Packard in Roseville, CA for 5 years as research engineer. Since 2001 he is a faculty member at the University Missouri Rolla in the Electromagnetic Compatibility group. His current research includes the development of measurement systems, High speed electronics design, Signal Integrity and Electromagnetic Compatibility.